

# DC current sensor using switching-mode excited in-situ current transformer

Václav Grim, Pavel Ripka, Jan Bauer

Faculty of Electrical Engineering, Czech Technical University, Prague 16627, Czech Republic  
(e-mail: vaclav.grim@fel.cvut.cz)

**Abstract**—DC current component in the power grid may cause gross measurement errors and lead to overheating of power transformers. We have previously developed method how to measure DC current using fluxgate effect in existing current transformers. In this paper we show that using ferroresonance the power consumption of such device can be drastically reduced. The microprocessor can both control the H-bridge excitation unit and perform signal processing, avoiding the need of external instruments.

**Index Terms**—Current sensor, current transformer, ferroresonance

## I. INTRODUCTION

DC currents in the grid may be caused by geomagnetic induction: DC current spikes up to 200 A with 3 minutes duration are observed during geomagnetic storms [1]. Another sources of DC current component are switching transients and uncompensated transformerless inverters, which are now standard in solar and wind power plants [2]. Novel source of “DC induction” through ground potentials are DC power transmission lines [3]. There is also a possibility of deliberate usage of half wave rectifiers for large loads, for the purpose of lowering the measured energy consumption: the half-way rectified current contains large DC current component, which partly saturates current transformer in the energy meter. The resulting error is always negative.

The current transformer (CT) are still the most popular devices for industrial applications [4]. CTs are susceptible to measurement errors caused by DC component in the measured (primary) current [5] and remanence [6] and also by magnetization from external fields. In order to avoid these gross errors, 2 types of DC tolerant current transformers has been developed: linear dc tolerant current transformers and dual-core current transformers.

Dual-core CTs have one core with high permeability for achieving low error and second core with low permeability and high DC immunity. While this combination works well for resistive loads, it fails for loads with inductive or capacitive character. The reason is rapid change of phase error when the high-permeability core is saturated. This leads to the gross error of measured power for loads with lower power factor [7].

Linear dc tolerant current transformers are usually made of nanocrystalline material with perpendicular anisotropy induced by field annealing [8] or by stress annealing [9]. Due to the perpendicular anisotropy the B-H characteristics is flat, with decreased permeability and high linearity, and with increased saturation field. Thanks to high saturation field the core is more resistant to saturation. Thanks to linear characteristics, the phase error is small; the amplitude error caused by decreased

permeability can be easily compensated [4].

However, most of the precise CTs installed in the grid are based on permalloy, with very low DC current immunity. Replacing them would be extremely expensive. Methods of improvement of accuracy of these transformers in the presence of DC current and means to measure this DC current component are therefore highly desired by the industry.

We have shown that DC currents can be measured with 5 % accuracy by existing CTs using additional AC excitation and detection of the second harmonic of the excitation frequency using the fluxgate principle [10].

There are three main reasons why it is important to measure DC current component in the grid:

1. To detect excessive level of DC current component which cause gross measurement errors or may cause saturation of power transformers and overheating
2. To act as zero indicator for the DC compensation scheme for transformerless power inverters
3. To feedback-compensate primary DC current component of current transformer to restore its accuracy for measuring of AC currents.

DC current comparators work on the similar principle as our device, but they require three windings: excitation, detection and feedback. DC current comparators also have two toroidal cores excited in opposite direction, so that the net AC flux is ideally zero and no current on excitation frequency is injected into the primary circuit [11]. Our simple device has many disadvantages which will be discussed later, but one very important advantage: it requires only single winding and single core so that it can use current transformers already installed in million volumes within the power grid. We cannot use autooscillation circuit such as described in [12] because we have to keep the secondary burden constant in order to maintain the AC operation of the CT.

First disadvantage of active DC current transformer which we developed and described in [10] is its complicated electronics and large power consumption of 391 W from 230V grid (324 W for the power amplifier, 23 W for the generator and 44 W for the lock-in amplifier). The CTs can be demagnetized

Accepted manuscript

V. Grim, P. Ripka, J. Bauer: DC current sensor using switching-mode excited in-situ current transformer, JMMM Vol. 500 (2020) 166360 doi.org/10.1016/j.jmmm.2019.166370

by momentarily increasing its burden by using pulse width modulation (PWM) switchable resistor [13]. PWM (Class D amplifier) has been also used for feedback compensation of current transducer [14]. This type of amplifier has very high efficiency, but suffer of the large ripple. Class H amplifier is a more complicated solution, but without the problem of ripple [15].

Similar technique was used in [16] for measuring and compensation of the DC bias in AC grid voltage. Measuring DC voltage instead of current is complementary approach which is very challenging: DC bias of 1 mV in 400 V grid may already cause serious saturation of the distribution transformer. Such small DC component can be measured by using all-even harmonics detection of the magnetization current of the saturable reactor [16].

In this paper we use excitation circuit to inject AC into the CT's secondary winding. Then we are able to measure DC component of the primary current by monitoring the second harmonic current in the secondary winding. The advantage of our method is that in can be used in-situ on current transformers already installed in the grid.

## II. CURRENT TRANSFORMER WITH SIMULATED SINEWAVE EXCITATION

In this mode we use sine wave excitation voltage in a way similar to [10], but in order to lower the energy consumption, we replaced the analog power amplifier by a hard-switched H-bridge. Sigma-delta bitstream controls the switching of one half of the bridge (Q3 and Q4), the other half (Q1 and Q2) is toggled only once per half-period based on polarity of the generated sine wave. This is done in order to reduce switching losses and switching noise.

### A. Circuit description

Simplified schematic diagram of the proposed circuit is shown in Fig. 1. The current transformer elaborated in this paper is Norma 179, rated at 400A primary and 5A secondary current with nominal burden of 0.2  $\Omega$ . On-state resistance of the switches must not significantly affect the total burden resistance defined by  $R_{\text{burden}}$ , therefore we chose IRFB4110 N-channel MOSFETs with  $R_{\text{DS(on)}}=4.5$  m $\Omega$ . Gate currents were provided by HIP4081A gate driver. All control and synchronization signals were generated by a Cortex-M4 MCU (NXP MK20) running at 72 MHz. Software-based delta-sigma modulator was used to generate a 43 Hz sine wave with a modulation frequency of 100 kHz. The H-bridge together with a digital delta-sigma modulator form a high power DAC. The amplitude and waveform of the AC component is controlled by a numerically controlled oscillator ( $f_{\text{drive}}$  in figure 1).

### B. Measurement methodology and results

Measured signal is extracted from voltage drop across the 0.1  $\Omega$  burden resistor using a HF2LI benchtop lock-in amplifier. The circuit can be operated in two modes. In passive mode Q1, Q4 are permanently on and Q2, Q3 off. This corresponds to conventional operation of a CT. Active mode is used for the measurement of DC primary current. In this case the H bridge

is switched to add AC component into the CT secondary winding.

The DC component of the current  $I_{\text{PRI}}$  can be measured from 2nd harmonics of the injected current. Fig. 2 shows the generated sine wave and resulting excitation current waveform.

While 43 Hz excitation frequency is sufficient for detection of DC current component, measuring 50 Hz current requires to increase excitation frequency - we have selected 237 Hz excitation for this purpose.

### C. Power consumption

The advantage of this solution is that the power consumption is only 30 W from 230 V grid (VCC1 + microprocessor + gate driver).

Net current consumption for 43 Hz is 20 mA from 5 V for bridge voltage, 18 mA from 5V for MCU and current sense amplifier, 33 mA from 12 V for gate driver.

However, net current consumption for 237 Hz excitation frequency is dramatically increased: 236 mA from 26 V for bridge voltage, 18 mA from 5 V for MCU and current sense amplifier, 33 mA from 12 V for gate driver. Additional issues include non-linearity of its transfer characteristics and rather complicated control. We therefore decided to use the ferroresonant mode.

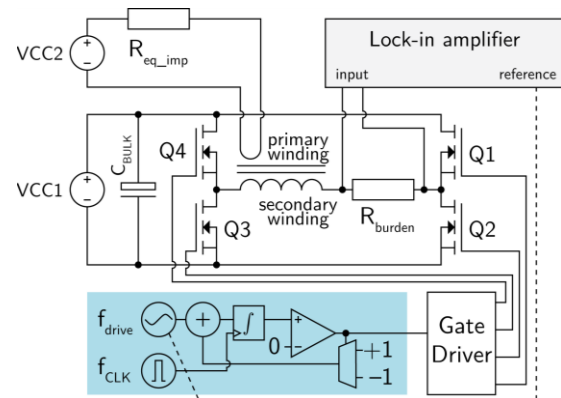


Fig. 1: Switched DC current transformer. Shaded rectangle denotes software-emulated digital circuitry.

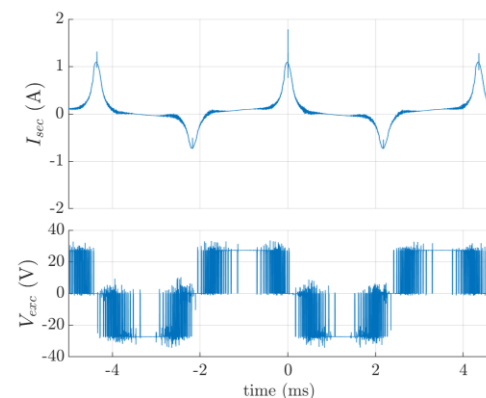


Fig. 2: Excitation voltage for unipolar switching (lower trace) simulating 43 Hz sine wave and corresponding excitation current (upper trace)

### III. CURRENT TRANSFORMER WITH SERIES RESONANT EXCITATION

The nonlinear LC excitation tank was described for fluxgate sensors and sinewave excitation in [17], for squarewave excitation by [18] and [19]. We have used the same ferroresonant circuit to achieve large excitation current peaks into the secondary or the CT while keeping the excitation power low. The circuit behavior is complex due to large nonlinearities, and the resonant mode is self-sustaining only over a certain range of supply voltage  $VCC_1$ .

#### A. Principle of operation

This resonant method uses the same hardware setup as the sine wave method with the exception of added 10  $\mu\text{F}$  capacitor  $C_{RES}$  (Fig. 3). The H-bridge creates a rectangular voltage waveform, which causes large resonant peaks of current through the secondary winding (Fig. 5).

The DC primary current causes large unbalance of the excitation current as shown in Fig. 5. Current unbalance can be observed at all even harmonics. The response for first six even harmonics is shown in Fig. 6. Even though its relatively low sensitivity, 2<sup>nd</sup> harmonic was selected for our implementation as it has the best linearity, which is important for open-loop operation. In case of feedback compensated mode the linearity is not critical and all-even harmonics approach can be used similarly as in [15b].

The disadvantage is that this mode does not allow feedback compensation by using the same switching transistors, as the serial capacitor blocks DC current component in the secondary winding. However, the sensor characteristics is linear even without compensation (linearity error is only 0.4 % for current up to 6 A) as shown in Fig. 7. The DC current range is limited to 16 A, for larger current the resonant mode is extinguished.

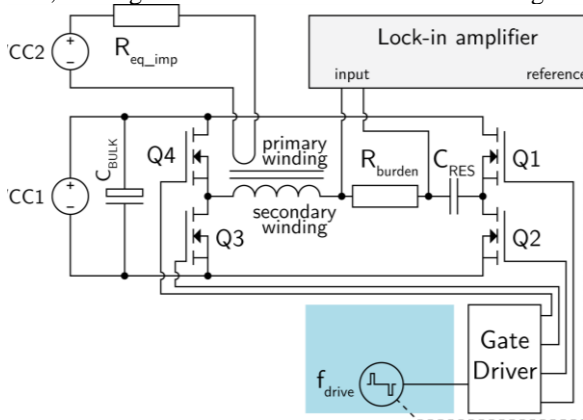


Fig. 3: Serial excitation resonant circuit. Shaded rectangle denotes internal operation of the controlling MCU.

#### B. Iron losses estimation

The power consumption in the resonance mode is expected to be reduced. However, the power consumed from 230 V grid is the same 30 W as in the simulated sinewave mode. The main advantage of the resonant mode is reduced supply voltage which allows to increase the excitation frequency without significant increase of net power consumption. The bridge

supply current from 9 V source was 180 mA (compare with 236 mA from 26 V for simulated sinewave).

The dynamic hysteresis loop (Fig. 4) shows that the excitation peaks guarantee deep saturation of the core material, which is vital to achieve low remanence and wide range. The hysteresis loop was measured by sampling H and B. H was derived from the 50 Hz current flowing through the 40-turn auxiliary primary winding and B was calculated from the integrated induced voltage at 80-turn secondary winding. The main single-turn primary winding was connected to Kepco BOP power supply in constant voltage mode through a 0.7  $\Omega$  resistor to provide DC bias current. Sampling was made by Agilent MSO3012 oscilloscope in high resolution mode. Integration and averaging of 10 periods was done during post-processing. In order to find the axis scale we have measured the core dimension using X-ray tomography: the core internal/external diameters are  $d_1 = 57.56\text{mm}$ ,  $d_2 = 81.42\text{mm}$ , and height  $h = 30.18\text{mm}$ . Stacking factor was estimated at 0.9. The hysteresis losses for can be derived from the same hysteresis loop as

$$P_{hyst} = fV \oint HdB$$

where  $f$  the excitation frequency and  $V$  is the core volume. From Fig. 4 we can estimate that for sinewave excitation the work done during one magnetization cycle is 20 J/m<sup>3</sup>, which for the volume of 0.00008 m<sup>3</sup> and 275 Hz frequency makes hysteresis power loss of only 0,44 W.

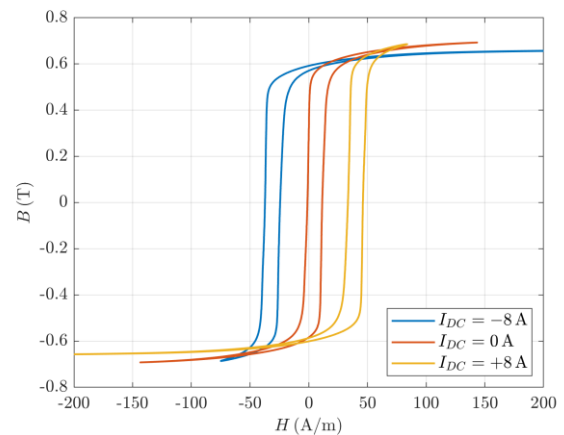


Fig. 4 Working hysteresis loop

#### C. Experimental results

The switching timing is shown in Fig. 5. The excitation current has a form of narrow peaks with repetition frequency of 237 Hz and 6 A p-p amplitude, which corresponds to  $H_{max} = 80 \cdot 3 \cdot \pi / 0.22 = 3400 \text{ A/m}$  for zero DC current in primary.

Figure 6 shows the first six even harmonics of excitation current versus the primary DC current. The 2nd harmonics has lowest sensitivity, but largest linear range: for 8 A current the linearity error is already 20%. Figure 7 shows linearity error in 5 A range for 2nd and 4th harmonics: in the 4A range the linearity error of 2nd harmonics is only  $\pm 0.2\%$ , while for the 4th harmonics this error is  $\pm 1.5\%$ . For the open-loop operation we have selected 2nd harmonics because it has the lowest linearity error. For the feedback-compensated mode a sum of

Accepted manuscript

V. Grim, P. Ripka, J. Bauer: DC current sensor using switching-mode excited in-situ current transformer, JMMM Vol. 500 (2020) 166360 doi.org/10.1016/j.jmmm.2019.166370

all even harmonics would give the best results in term of sensitivity.

An important feature of this mode is low dependence of the sensitivity on impedance in the primary circuit (Fig. 8).

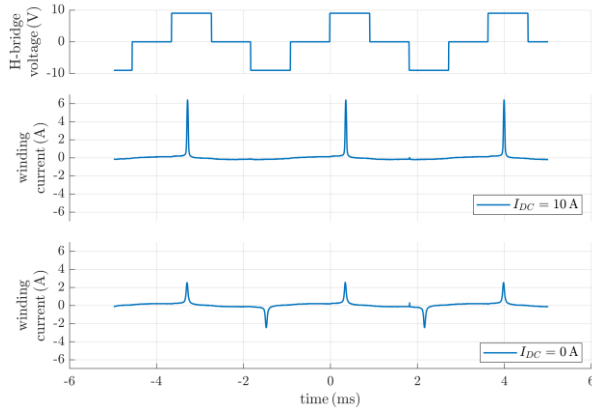


Fig. 5: Excitation current for different values of DC primary current

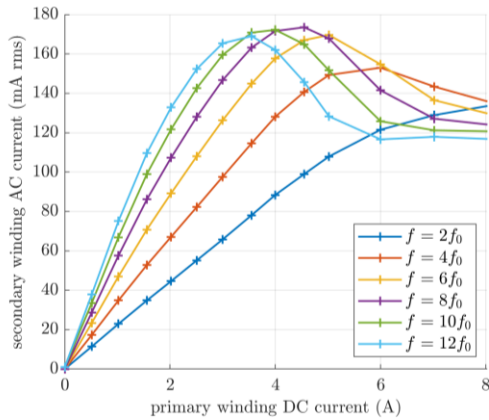


Fig. 6 Even harmonic response of the excitation current to the DC primary current

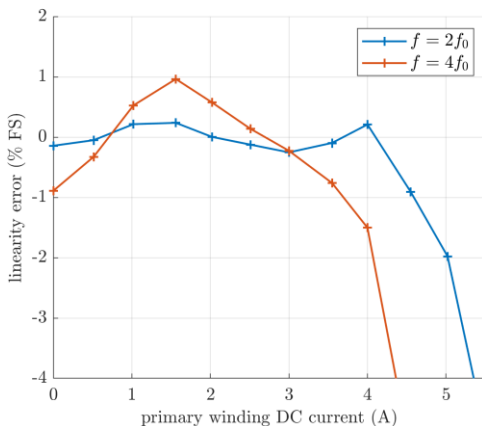


Fig. 7 Measured non-linearity for second and fourth harmonics

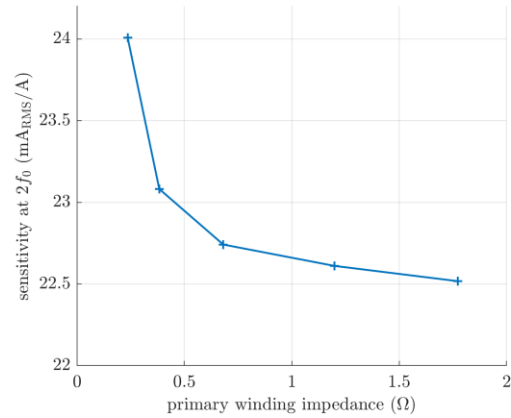


Fig. 8 Second harmonic sensitivity as a function of the impedance in primary circuit

In order to evaluate resolution we measured noise spectra of 2nd and 4th harmonics signals (Fig. 9). The noise spectrum density is  $20 \mu\text{A}/\sqrt{\text{Hz}}$  at 1 Hz for 2nd harmonics and slightly lower value for 4th harmonics. The noise in the 100 mHz to 3 Hz frequency band is below  $50 \mu\text{A rms}$ .

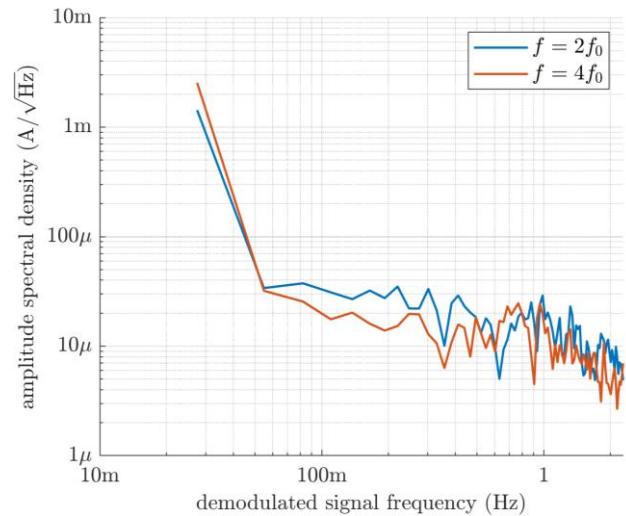


Fig. 9 Spectrum of demodulated signal, second and fourth harmonics

#### D. Current injected into the primary conductor

Excitation current appears also in the primary circuit due to the (current) transformer effect. This is illustrated in Fig. 9. Secondary winding was driven with  $10 \text{ A}_{\text{PP}}$  pulses. The injected current is large for short-circuited primary: for  $R_1 = 100 \text{ m}\Omega$  impedance in the primary circuit the injected current is  $I_{\text{exc}} = 6.2 \text{ A p-p}$ . However, the injected current is acceptable for realistic grid impedance: for  $R_1 = 1.8 \Omega$  the injected current is  $I_{\text{exc}} = 350 \text{ mA p-p}$ .

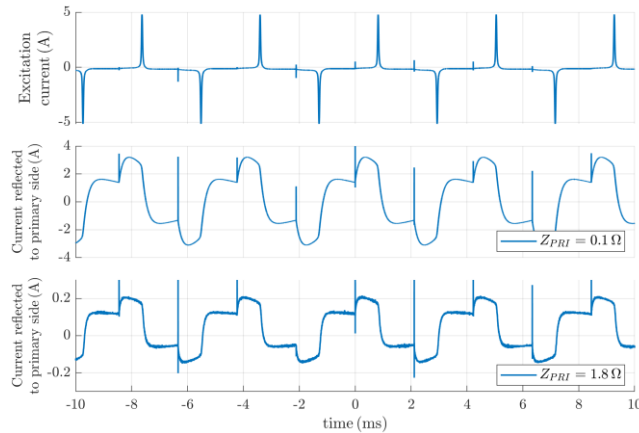


Fig. 9: Series resonance mode: excitation current (top trace), AC current injected into the primary circuit  $I_{exc}$  for primary impedance  $R_1 = 100 \text{ m}\Omega$  (middle trace) and for  $R_1 = 1.8 \Omega$  (bottom trace)

#### E. Response to AC primary current

The secondary current  $I_2$  response to 50 Hz primary current  $I_1$  is shown in Fig. 10. Signal from the primary side modulates the excitation waveform. Due to large nonlinearity the frequency spectrum of  $I_2$  is very rich, containing multiples of mains frequency (50 Hz) and excitation frequency (237 Hz) and their modulation products. The amplitude of the 50 Hz primary current can be measured from these modulation products, however the accuracy is low compared with standard CT operation. The final instrument is therefore expected to operate in active driving mode (Mode 2) only for short periods and most of the time remain in ordinary AC-only passive mode (Mode 1).

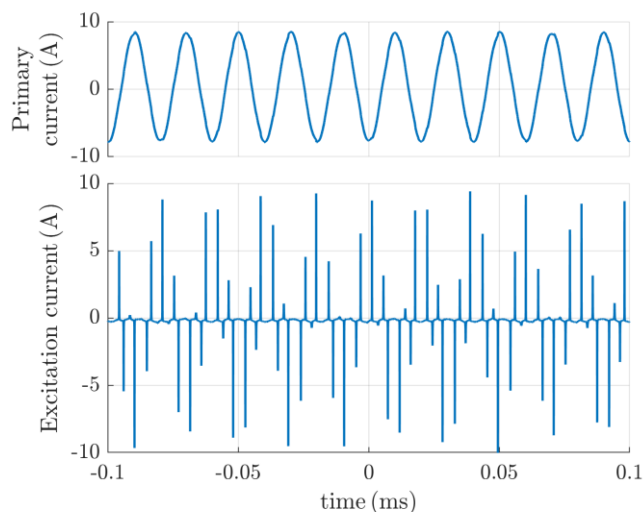


Fig. 10 Response of the secondary current to 16 A<sub>pp</sub> primary current

#### IV. PARALLEL RESONANCE EXCITATION MODE

The parallel excitation circuit is shown in Fig. 11. Instead of using current generator it is enough to increase the impedance of the excitation source by serial resistance or inductance.

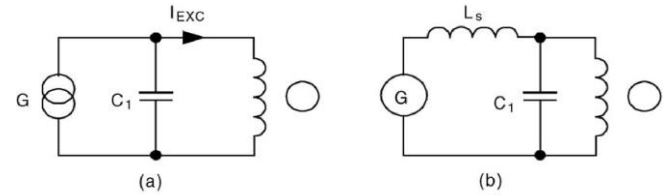


Fig. 11: Parallel excitation circuit a) idealized b) implemented by choke in series [17]

We have tested this operation mode with serial inductance  $L_s = 20 \text{ mH}$  in series with  $R_s = 14 \Omega$ . The achieved excitation parameters were similar as for the serial mode, however the circuit was more sensitive to impedance in the primary circuit.

#### V. CONCLUSION

We have developed compact microprocessor-controlled instrument, which can be used with existing current transformer to add the functionality of DC current measurement and compensation. The power consumption depends on the measurement mode and used CT. As the DC currents in the real grid are changing only slowly, sampling time of 1 s and measurement time of 100 ms will be sufficient. Thus the 90 % of the time the transducer works in the classical CT mode, making only negligible compromise for AC accuracy.

For 400A/5A, 5VA CT we have demonstrated open-loop DC measurement range of 8 A, with (maximum) linearity error of 20 %. For the currents below 4 A the linearity error is below 0.2 %. The linearity can be further improved by using feedback compensation. The current resolution is 50  $\mu\text{A}$  (noise power spectrum density PSD = 20  $\mu\text{A}/\sqrt{\text{Hz}}$  at 1 Hz) The power consumption for 10% duty cycle will be below 0.5 W. Even though the instrument uses only a single core, it injects only 350 mA p-p into the primary circuit. The last advantage is that the response to the primary current is linear and does not depend on the grid impedance. Because of that the feedback compensation of the primary DC current is only necessary if high accuracy is required.

#### ACKNOWLEDGMENT

This study was supported by the Grant Agency of the Czech Republic within the New Methods for the Measurement of Electric Currents” project (GACR 17-19877S).

#### REFERENCES

- [1] Kasztenny, B., N. Fischer, D. Taylor, T. Prakash, and J. Jalli. 2016. "Do CTs Like DC?." 69th Annual Conference for Protective Relay Engineers, College Station, Texas.
- [2] Buticchi, G., E. Lorenzani, and G. Franceschini. 2011. "A DC Offset Current Compensation Strategy in Transformerless Grid-Connected Power Converters." IEEE Transactions on Power Delivery 26 (4): 2743-2751. doi 10.1109/tpwr.2011.2167160.
- [3] S. H. Yang, G. Zhou, and Z. N. Wei, "Influence of High Voltage DC Transmission on Measuring Accuracy of Current Transformers," IEEE Access, vol. 6, pp. 72629-72634, 2018.
- [4] P. Ripka: Contactless measurement of electric current using magnetic sensors, Technisches Messen 2019, Early Access doi 10.1515/teme-2019-0032

V. Grim, P. Ripka, J. Bauer: DC current sensor using switching-mode excited in-situ current transformer, *JMMM* Vol. 500 (2020) 166360 doi.org/10.1016/j.jmmm.2019.166370

- [5] Mlejnek P., Kaspar P., DC tolerance of current transformers and its measurement, *Journal of Electrical Engineering*, Vol. 57, No. 8/S (2006), 48–50
- [6] K. Draxler, and R. Styblikova, "Demagnetization of instrument transformers before calibration," *Journal of Electrical Engineering-Elektrotechnicky Casopis*, vol. 69, no. 6, pp. 426-430, Dec, 2018.
- [7] P. Mlejnek, and P. Kaspar, "Drawback of Using Double Core Current Transformers in Static Watt-Hour Meters," *Sensor Letters*, vol. 7, no. 3, pp. 394-396, Jun, 2009.
- [8] Pluta, W., C. Swieboda, J. Leszczynski, and M. Soinski. 2017. "Some remarks on metrological properties and production technology of current transformers made of nanocrystalline cores." *Measurement* 97: 38 - 44. <https://doi.org/10.1016/j.measurement.2016.11.024>.
- [9] Gunther, W. 2005. "Stress annealing process suitable for the production of low permeable nanocrystalline tape wound cores." *J. Magn. Mag. Mat.* 290: 1483-1486. Doi 10.1016/j.jmmm.2004.11.555.
- [10] P. Ripka, K. Draxler, R. Styblikova: DC-compensated Current Transformer, *Sensors* 16 (2016), 114
- [11] P. Ripka, Electric current sensors: a review, *Meas. Science and Technology* 21 (2010) Iss. 11, pp.1-23.
- [12] J. A. Cao, J. Zhao, and S. Cheng, "Research on the simplified direct-current fluxgate sensor and its demodulation," *Measurement Science and Technology*, vol. 30, no. 7, Jul, 2019.
- [13] J. Bauer, P. Ripka, K. Draxler, R. Styblikova: Demagnetization of Current Transformers Using PWM Burden, *IEEE Trans Magn* 51 (2015), Article#: 4000604.
- [14] S. Veinovic, M. Ponjavic, S. Milic et al., "Low-power design for DC current transformer using class-D compensating amplifier," *IET Circuits Devices & Systems*, vol. 12, no. 3, pp. 215-220, May, 2018.
- [15] G. Velasco-Quesada, M. Roman-Lumbreras, R. Perez-Delgado et al., "Class H Power Amplifier for Power Saving in Fluxgate Current Transducers," *IEEE Sensors Journal*, vol. 16, no. 8, pp. 2322-2330, Apr, 2016.
- [16] S. N. Vukosavic, L. S. Peric, "High-precision sensing of DC bias in ac grids", *IEEE Trans. Power Del.*, vol. 30, no. 3, pp. 1179-1186, Jun. 2015
- [17] P. Ripka, W.G. Hurley: Excitation efficiency of fluxgate sensors, *Sensors and Actuators A* 129 (2006), pp.75-79, <http://dx.doi.org/10.1016/j.sna.2005.09.047>
- [18] Cerman, A., Merayo, J. M. G., Brauer, P., Primdahl, F. (2008). Self-Compensating Excitation of Fluxgate Sensors for Space Magnetometers. *IMTC 2008*. IEEE. <https://doi.org/10.1109/IMTC.2008.4547387>
- [19] Liu S, Cao DP, Jiang CZ: A solution of fluxgate excitation fed by squarewave voltage, *Sens. Act. A* 163 (2010), 118-121, doi: 10.1016/j.sna.2010.08.003